

Title:

Simplified Spectropolarimetry Using Reactive Mesogen Polarization Gratings

Authors:

Michael J. Escuti, Chulwoo Oh, Carlos Sánchez, Cees W.M. Bastiaansen, and Dirk J. Broer

Affiliations:

North Carolina State University, Dept Electrical & Computer Engineering, Raleigh, NC (USA)
Universidad de Zaragoza, Dept de Física de la Materia Condensada, Zaragoza (Spain)
Eindhoven University of Technology, P.O. Box 513, 5600 MB Eindhoven (The Netherlands)
Philips Research Laboratories, Prof. Holstlaan 4, 5656 AA Eindhoven (The Netherlands)

Presented At:

SPIE Optics & Photonics Conference, San Diego, CA (August 13-17, 2006)

Citation:

M.J. Escuti, C. Oh, C. Sánchez, C.W.M. Bastiaansen, and D.J. Broer, "Simplified Spectropolarimetry Using Reactive Mesogen Polarization Gratings", *Proceedings of SPIE*, **vol. 6302**, no. 630207 (2006).

Copyright 2006 Society of Photo-Optical Instrumentation Engineers.

This paper was published in Proceedings of SPIE Vol. 6302 and is made available as an electronic reprint with permission of SPIE. One print or electronic copy may be made for personal use only. Systematic or multiple reproduction, distribution to multiple locations via electronic or other means, duplication of any material in this paper for a fee or for commercial purposes, or modification of the content of this paper are prohibited.

Simplified Spectropolarimetry Using Reactive Mesogen Polarization Gratings

Michael J. Escuti,^a Chulwoo Oh,^a Carlos Sánchez,^b Cees Bastiaansen,^c and Dirk J. Broer^{c,d}

^aNorth Carolina State Univ, Dept Electrical & Computer Engineering, Raleigh, NC (USA);

^bUniv de Zaragoza, Dept de Física de la Materia Condensada, Zaragoza (Spain);

^cEindhoven University of Technology, P.O. Box 513, 5600 MB Eindhoven (The Netherlands);

^dPhilips Research Laboratories, Prof. Holstlaan 4, 5656 AA Eindhoven (The Netherlands)

ABSTRACT

The measurement of complete polarimetric parameters for a broad spectrum of wavelengths is challenging because of the multi-dimensional nature of the data and the need to chromatically separate the light under test. As a result, current methods for spectropolarimetry and imaging polarimetry are limited because they tend to be complex and/or relatively slow. Here we experimentally demonstrate an approach to measure all four Stokes parameters using three polarization gratings and four simultaneous intensity measurements, with potential to dramatically impact the varied fields of air/space-borne remote sensing, target detection, biomedical imaging/diagnosis, and telecommunications. We have developed reactive mesogen polarization gratings using simple spin-casting and holography techniques, and used them to implement a potentially revolutionary detector capable of simultaneous measurement of full polarization information at many wavelengths with no moving or tunable elements. This polarimeter design not only enables measurements over a likely bandwidth of up to 70% of the center wavelength, it is also capable of measurements at relatively high speed (MHz or more) limited only by the choice of photo-detectors and processing power of the system. The polarization gratings themselves manifest nearly ideal behavior, including diffraction efficiencies of greater than 99%, strong polarization sensitivity of the first diffraction orders, very low incoherent scattering, and suitability for visible and infrared light. Due to its simple and compact design, simultaneous measurement process, and potential for preserving image registration, this spectropolarimeter should prove an attractive alternative to current polarization detection and imaging systems.

Keywords: polarimetry, spectropolarimetry, polarization grating, hyperspectral, multispectral, liquid crystals, reactive mesogens

1. INTRODUCTION

Various polarimeter designs based on polarization gratings have been proposed and tested,^{1,2,4-6} and offer a compelling route to real-time measurement of all four Stokes parameters⁷ across a broad wavelength range simultaneously. These promise to overcome the limitations in speed physical size, complexity, and alignment sensitivity of conventional space- and air-borne platforms developed for solar polarimetry, astronomy, remote sensing, and target detection.

Polarization gratings^{8,9} (PGs), sometimes called anisotropic or vectorial gratings, are embodied as a spatially varying birefringence and/or dichroism, and essentially operate by periodically modulating the polarization state of the wavefront passing through them (as opposed to modulating its phase or amplitude alone). Previous polarimetry approaches using PGs have faced limitations of photo- and temperature stability of the azobenzene-containing materials² and the need for involved parametric calibration.⁵ While one of the most recent works⁶ demonstrates the measurement of all four Stokes parameters with reasonable accuracy with only two diffraction gratings, it is limited by its need for two polarizers, and the photo-instability of its azo-based materials to green or blue light.

Correspondence should be addressed to: mjescuti@ncsu.edu, +1 919 513 7363

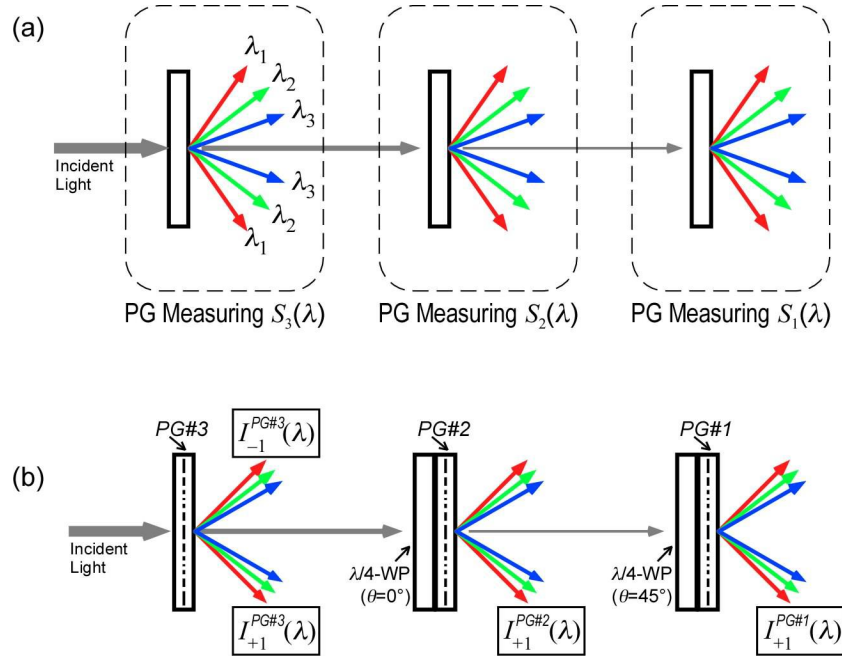


Figure 1. Spectropolarimetry using polarization gratings (PGs): (a) Basic idea of inline Stokes parameter detection; and (b) Our proposed implementation with three PGs and two quarter-waveplates enabling detection of the complete Stokes vector with only four *simultaneous* intensity measurements per wavelength. (color figure)

We suggest that an ideal spectropolarimeter would (*i*) determine the full Stokes vector through only four simultaneous intensity measurements per wavelength, (*ii*) require no polarizers at all (avoiding their expense, bulk, and wavelength limitations), (*iii*) offer the potential to operate across wavelengths ranging from $0.4 \mu\text{m}$ to mid-infrared with easy calibration, (*iv*) be robust to photo/mechanical/chemical/thermal degradation, and (*v*) have ability to be easily fabricated with clear apertures of several cm^2 or more. The inline PG spectropolarimeter we describe and validate here achieves all of these properties.

In what follows, we will introduce the theoretical basis of the proposed polarimeter using a Jones matrix approach, describe the fabrication and properties of our reactive mesogen PGs, and finally discuss the results of a representative validation experiment.

2. POLARIMETRY USING POLARIZATION GRATINGS

While the details of polarimetry using PGs depend on the specific implementation,²⁻⁶ a generic description capturing the basic elements of the approach is illustrated Fig. 1(a). An inline arrangement of polarization-sensitive diffraction gratings allows for the detection at each stage of at least one of the Stokes parameters by the measurement of the diffracted intensities. Wavelength separation occurs inherently (governed by the grating equation), and detection can be done in a fashion similar to conventional spectrometers using linear photodetector arrays or two-dimensional focal-plane-arrays. In this work, we utilize three PG elements along with two achromatic quarter-waveplates to implement the spectropolarimeter, as shown in Fig. 1(b).

One of the most important PG profiles is a continuous, in-plane, linear birefringence texture^{1,8,9} with a uniaxial optical anisotropy that follows the spatial profile $[\sin(\pi x/\Lambda), \cos(\pi x/\Lambda), 0]$, where Λ is the grating period. This is illustrated in Fig. 2(a) where the linear birefringence is embodied in a nematic liquid crystal director (fabrication to be discussed in Section 3). It has long been known that this anisotropic diffraction grating manifests a combination of the most advantageous properties of both thick-and thin-gratings (and beyond): 100% diffraction efficiency, strong polarization sensitivity of the ± 1 -order diffraction, polarization-independence of the 0-order diffraction, and comparatively wide bandwidth.

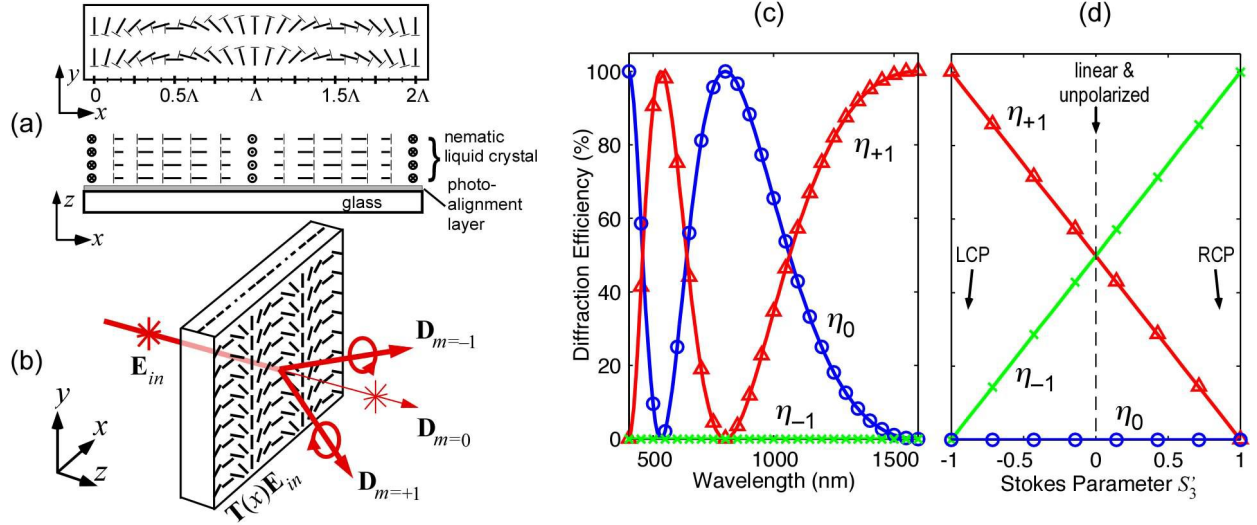


Figure 2. Structure and properties of the liquid crystal polarization grating (LCPG): (a) Top- and side-views of the continuous, in-plane configuration of the nematic LC with a periodic linear birefringence; (b) Ideal diffraction from the LCPG texture into only three possible orders; (c) Calculated diffraction efficiency of the 0- and ± 1 -orders with circularly polarized input light ($\Delta nd = 800$ nm), highlighting the potential for 100% diffraction into a single order; and (d) Calculated polarization sensitivity (at $\Delta nd/\lambda = 1/2$) to the Stokes parameter quantifying ellipticity ($S'_3 = S_3/S_0$). (color figure)

In what follows, we derive a concise summary of the properties of this PG element, based in part on Jones-matrix reasoning.^{8,10–12} We begin by assuming an infinite grating and express the (far-field) electric field \mathbf{D}_m for each diffraction order m as the Fourier transform of the (near-field) output. In the paraxial approximation¹³ (when $2\pi\lambda d/n_0\Lambda^2 < 1$), local electric field after the PG can be expressed as the input electric field $\mathbf{E}_{in} = [E_x, E_y]^T$ transformed by the local Jones matrix of the anisotropic grating $\mathbf{T}(x)$ such that the near-field output is $\mathbf{T}(x)\mathbf{E}_{in}$. Under this set of assumptions, illustrated in Fig. 2(b), we can express the far-field electric field of the diffraction order m as follows:

$$\mathbf{D}_m = \frac{1}{\Lambda} \int_0^\Lambda \mathbf{T}(x)\mathbf{E}_{in} \exp(-i2\pi mx/\Lambda) dx, \quad (1)$$

where Λ is half the nematic period as defined in Fig. 2(a), $\mathbf{T}(x) = \exp(i\pi\Delta\mathbf{n}(x)d/\lambda)$ is the spatially-varying 2×2 Jones transfer matrix of the PG, $\Delta\mathbf{n}(x)$ is the birefringence tensor describing the local uniaxial anisotropy, and λ is the wavelength of incident light. For the continuous, in-plane, linear birefringence texture of this PG, the transfer matrix^{8,10,12} is

$$\mathbf{T}(x) = \cos \zeta \mathbf{I} + i \sin \zeta \begin{bmatrix} \sin(2\pi x/\Lambda) & \cos(2\pi x/\Lambda) \\ \cos(2\pi x/\Lambda) & -\sin(2\pi x/\Lambda) \end{bmatrix}, \quad (2)$$

where $\zeta = \pi\Delta nd/\lambda$ is the normalized local retardation, Δn is the birefringence of the LC, d is the thickness of the birefringent layer, \mathbf{I} is the identity matrix, and where the absolute phase has been neglected.

Since the incident electric field does not depend on x , we can rewrite Eq. 1 as

$$\mathbf{D}_m = \mathbf{\Gamma}_m \mathbf{E}_{in}, \quad (3)$$

where the *grating transfer matrix* is defined as $\mathbf{\Gamma}_m = \Lambda^{-1} \int_0^\Lambda \mathbf{T}(x) \exp(-i2\pi mx/\Lambda) dx$. For the purpose of this work, $\mathbf{\Gamma}_m$ completely describes the effect of a single PG, relating the Jones vector of diffracted light to the incident Jones vector according to Eq. 3. The grating transfer matrix for the LCPG has non-zero solutions only for $|m| \leq 1$:

$$\mathbf{\Gamma}_0 = \cos \zeta \mathbf{I}, \quad (4)$$

$$\mathbf{\Gamma}_{\pm 1} = \frac{\sin \zeta}{2} \begin{bmatrix} \mp 1 & 1 \\ 1 & \pm 1 \end{bmatrix}. \quad (5)$$

We can now solve for the diffraction efficiency as the ratio of output to input intensity ($\eta_m = |\mathbf{D}_m|^2/|\mathbf{E}_{in}|^2$):

$$\eta_0 = \cos^2 \left(\frac{\pi \Delta nd}{\lambda} \right) \quad (6)$$

$$\eta_{\pm 1} = \frac{1}{2} (1 \mp S'_3) \sin^2 \left(\frac{\pi \Delta nd}{\lambda} \right) \quad (7)$$

where $S'_3 = S_3/S_0$ is the normalized Stokes parameter corresponding to ellipticity of the incident light.

Several unique and useful properties are included in Eqs. 6 and 7. *First*, note that 100% diffraction efficiency into one of the first-orders is possible when input light is circularly-polarized and when the effective PG retardation is halfwave ($\Delta nd = \lambda/2$). This is true even though the grating can be considered "thin" from the coupled-wave perspective. The simulated transmission spectra for the 0- and ± 1 -orders is shown in Fig. 2(c) for a grating optimized for maximum efficiency at $\lambda = 1600nm$. *Second*, the efficiencies of the ± 1 -orders are highly sensitive to the polarization (i.e. ellipticity) of incident light. To highlight this, we plot diffraction efficiency for the entire range of the normalized Stokes parameter S'_3 (Fig. 2(d)) for the case of $\Delta nd = \lambda/2$. Note that when incident light is linearly polarized or unpolarized, $S'_3 = 0$ and the diffraction efficiency in each first-order efficiency will be 50%. *Third*, as can be seen from Eq. 4, light passing directly through (0-order "diffraction") will have the same polarization state as the incident light.

It should be clear that these three unique properties make it suitable to implement the first element in Fig. 1(b), allowing the measurement of both S_3 and S_0 for each wavelength knowing only the parameters of the PG and the first-order intensities $I_{+1}(\lambda)$ and $I_{-1}(\lambda)$. Additionally, we have discovered that this PG may also be configured to measure the other two Stokes parameters when combined with achromatic quarter-waveplates, enabling a simple implementation of the second two elements in Fig. 1.

Consider the assembly in Fig. 1(b), where the second stage is implemented as a quarter-waveplate (symmetry axis parallel to the X-axis ($\theta = 0^\circ$)) placed immediately before the PG. The Jones transfer matrix for a quarter-waveplate at an angle θ from the X-axis can be expressed⁷ as

$$\mathbf{J}_{\lambda/4}^\theta = \frac{1}{\sqrt{2}} \begin{bmatrix} 1 + i \cos 2\theta & i \sin 2\theta \\ i \sin 2\theta & 1 - i \cos 2\theta \end{bmatrix}. \quad (8)$$

If we consider this assembly in isolation (apart from the first stage), the electric-field of the diffracted orders can be found as a function of the light incident on the quarter-waveplate:

$$\mathbf{D}_{\pm 1} = \mathbf{\Gamma}_{\pm 1} \mathbf{J}_{\lambda/4}^{0^\circ} \mathbf{E}_{in} = \frac{\sin \zeta}{2\sqrt{2}} \begin{bmatrix} \mp(1+i) & 1-i \\ 1+i & \pm(1-i) \end{bmatrix} \mathbf{E}_{in}. \quad (9)$$

The diffraction efficiency of this quarter-waveplate ($\theta = 0^\circ$) and PG assembly is therefore

$$\eta_{\pm 1} = \frac{1}{2} (1 \pm S'_2) \sin^2 \left(\frac{\pi \Delta nd}{\lambda} \right), \quad (10)$$

where $S'_2 = S_2/S_0$ is the normalized Stokes parameter corresponding to the component of incident light linearly polarized in the $\pm 45^\circ$ directions. The 0-order diffraction efficiency η_0 is the same as Eq. 6.

Finally, consider an assembly with two quarter-waveplates placed immediately before the PG. If the first waveplate has its symmetry axis at 0° and the second at 45° , the electric-field of the diffracted orders can be expressed as

$$\mathbf{D}_{\pm 1} = \mathbf{\Gamma}_{\pm 1} \mathbf{J}_{\lambda/4}^{45^\circ} \mathbf{J}_{\lambda/4}^{0^\circ} \mathbf{E}_{in} = \frac{\sin \zeta}{4} \begin{bmatrix} (-1 \mp 1 + i \mp i) & (1 \mp 1 - i \mp i) \\ (1 \mp 1 + i \pm i) & (1 \pm 1 + i \mp i) \end{bmatrix} \mathbf{E}_{in}. \quad (11)$$

The diffraction efficiency of this double-waveplate ($\theta = 0^\circ, 45^\circ$) and LCPG assembly is therefore

$$\eta_{\pm 1} = \frac{1}{2} (1 \mp S'_1) \sin^2 \left(\frac{\pi \Delta nd}{\lambda} \right), \quad (12)$$

where $S'_1 = S_1/S_0$ is the normalized Stokes parameter corresponding to the component of incident light linearly polarized in the horizontal and vertical directions. The 0-order diffraction efficiency η_0 is the same as Eq. 6.

All four Stokes parameters can be found using the spectropolarimeter illustrated in Fig. 1(b) by measuring four intensities at each wavelength:

$$\begin{bmatrix} S_0(\lambda) \\ S_1(\lambda) \\ S_2(\lambda) \\ S_3(\lambda) \end{bmatrix} = \begin{bmatrix} 0 & 0 & C & C \\ -A & 0 & C & C \\ 0 & B & -C & -C \\ 0 & 0 & C & -C \end{bmatrix} \begin{bmatrix} I_{+1}^{PG\#1}(\lambda) \\ I_{+1}^{PG\#2}(\lambda) \\ I_{+1}^{PG\#3}(\lambda) \\ I_{-1}^{PG\#3}(\lambda) \end{bmatrix} \quad (13)$$

with

$$\begin{aligned} A &= 2(T \sin^2 \zeta_1 \cos^2 \zeta_2 \cos^2 \zeta_3)^{-1} \\ B &= 2(T^2 \sin^2 \zeta_2 \cos^2 \zeta_3)^{-1} \\ C &= 2(T^3 \sin^2 \zeta_3)^{-1} \end{aligned}, \quad (14)$$

where the subscripts refers to the parameters of the respective PG ($\zeta_1 = \pi \Delta n_1 d_1 / \lambda$, $\zeta_2 = \pi \Delta n_2 d_2 / \lambda$, $\zeta_3 = \pi \Delta n_3 d_3 / \lambda$). The factor T is the total transmittance of each PG stage, which includes the influence of the material absorption and Fresnel reflection losses at the interfaces. We assume here that this factor is the same for each PG stage.

In this section, we have shown how all four Stokes parameters may be determined from four *simultaneous* intensity measurements per wavelength and a simple calculation (Eq. 13). In the next Section, we consider the fabrication of a robust, efficient, and high-quality PG element.

3. REACTIVE MESOGEN POLARIZATION GRATINGS

Until now, there has been no way to fabricate practical PGs with high efficiency, low optical scattering, and robust stability for the entire range of visible and near-infrared wavelengths. The most popular approach using holography with organic materials containing azobenzene moieties^{11,14-16} can have modest diffraction efficiencies¹⁵ (80%) and a wide range of grating periods.¹⁷ However, it is limited by absorption at visible wavelengths and irreversible degradation when illuminated or when heated above modest temperatures. No other bulk holographic material¹⁸ or lithographic technique¹⁹ achieves all three properties either.

An alternative approach employs patterned surfaces which then transfer their anisotropy to a liquid crystal (LC) layer.²⁰⁻²² While all of the early approaches²¹⁻²⁶ involved binary patterning with limited results, several groups^{20,27,28} recognized that a continuous LC diffractive grating would have improved diffraction properties. The foundational experimental results^{20,29} were promising, but were plagued by pervasive defects crippling their optical properties due to poor LC alignment, particularly in the LC-polymer PG case.²⁹ Consequently, the maximum diffraction efficiency was low, polarization sensitivity was far less than ideal, and strong incoherent scattering outside of the diffraction orders was present.

We have recently experimentally realized defect-free PGs with ultra-high efficiency and low scattering. Fabrication proceeds with four basic steps illustrated in Fig. 3(a). *First*, a glass substrate is coated with a photo-alignment material.³⁰ This layer is a thin photo-sensitive polymer film that manifests a strong orientational photo-chemical reaction in response to the local direction of linearly polarized UV light.^{30,31} In the work described here, we utilize ROP-103/2CP (Rolic Technologies Ltd.). *Second*, the substrate is exposed to a polarization hologram^{8,12} from an ultraviolet laser. This is formed by two coherent beams from a laser (Ar⁺, 351 nm, dose = ~ 8 J/cm²) with orthogonal circular polarizations that are superimposed with a small angle between them, leading to an interference pattern with constant intensity and a periodically varying linear polarization state that follows Fig. 1(a) (with period $\Lambda = \lambda_R / 2 \sin \Theta$, where λ_R is the recording wavelength and Θ is the half the angle between the beams). *Third*, a reactive mesogen mixture is coated on the photo-alignment layer, and made to align according to the surface pattern (typical spin-speed 2 krpm for 30 s, then baked at 65°C for 30 s). LC monomers (often called reactive mesogens) are low molecular-weight LCs (e.g. as in Fig. 3(b)), that can be polymerized to form high-molecular weight structures.³²⁻³⁴ Their orientation can be controlled by surfaces and

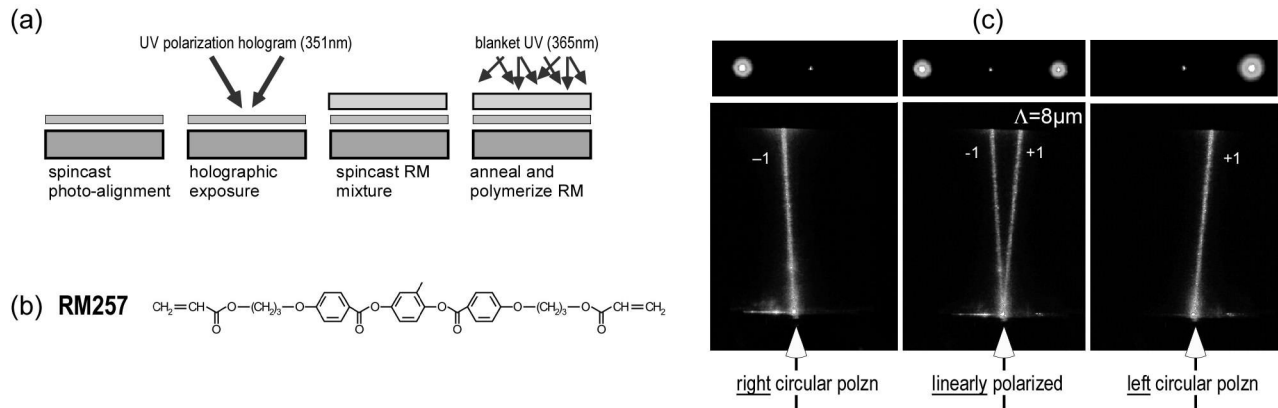


Figure 3. Fabrication of the reactive mesogen polarization grating (PG): (a) The four primary steps, including standard thin-film processing and ultraviolet (UV) holography; (b) Reactive mesogen molecule RM257 (Merck) used here as the primary element in our LC mixtures; and (c) Photographs of the resulting diffraction from our reactive mesogen PGs, highlighting the high diffraction efficiency, low scattering, and strong sensitivity to the polarization state of input light (monochromatic at 633 nm).

electromagnetic fields, and sophisticated molecular architecture can thereby be permanently captured as a polymer film. We utilized custom mixtures of LC diacrylates RM257 and RM82 (Merck), ultraviolet photo-initiator, a fluorinated surfactant promoting planar alignment at the LC-air interface, and solvent PGMEA with relative concentrations 26.8/6.7/0.5/1.0/65 by weight. *Fourth*, the reactive mesogen layer is photo-polymerized with a blanket ultraviolet exposure to permanently fix the large structured optical anisotropy. Because these acrylate reactive-mesogens result in a densely cross-linked polymer, they are robust to optical, thermal, mechanical, and chemical degradation.³⁵

The resulting PG exhibits all the properties predicted by theory (Eqs. 7 and Fig. 1(b)) with unsurpassed fidelity. For example, a reactive mesogen PG was fabricated with grating period $\Lambda = 8 \mu\text{m}$ and thickness $d = 2.2 \mu\text{m}$ (matched to the half-wave retardation condition for a HeNe laser, 633 nm). Photographs of the diffraction are shown in Fig. 3(c), where only the 0- and ± 1 -orders are present, strong sensitivity to the ellipticity of the incident light is observed, and nearly ideal diffraction into the first orders occurs when the input is circularly polarized $\sim 99.6\%$. Incoherent scattering was very low ($< 0.1\%$) because we have overcome the disclination lines and random defects present in previous work.^{29,36} Note that we define the experimental diffraction efficiency as $\eta_m = I_m / (\dots + I_{-1} + I_0 + I_{+1} + \dots)$, where the effect of the hologram is isolated, and Fresnel (air-glass) reflection losses and ITO absorption are normalized out.

We quantitatively measured the polarization-dependent diffraction properties using the setup in Fig. 4(a), where a linearly polarized probe laser was arranged such that it would be modulated by the rotation of a waveplate. In Fig. 4(b) and 4(c), a quarter-waveplate was rotated to vary the probe light between circular and linear polarizations as the $+1$ - and -1 -order diffraction efficiencies were measured. An excellent match with Eq. 7 is observed. The polarization contrast ratio (between left and right handedness) in the first-orders was remarkably $> 4000 : 1$. The response to a half-waveplate was also measured, and revealed an almost constant $\sim 50\%$ for both first-orders regardless of the orientation of the input linearly polarized light (Fig. 4(d) and 4(e)), as expected.

4. POLARIMETRY EXPERIMENT

In order to prove the principle-of-operation of the proposed spectropolarimeter (Fig. 1), three reactive mesogen PGs with were prepared on borosilicate glass substrates. Their grating period ($\Lambda = 5 \mu\text{m}$) and birefringence (measured at $\Delta n \approx 0.144$ at 1550 nm) were the same for each, and the thicknesses were 6, 3, and 2 μm for PG#1, PG#2, and PG#3 respectively. The 0-order efficiency spectra are shown in Fig. 5, and each had an area

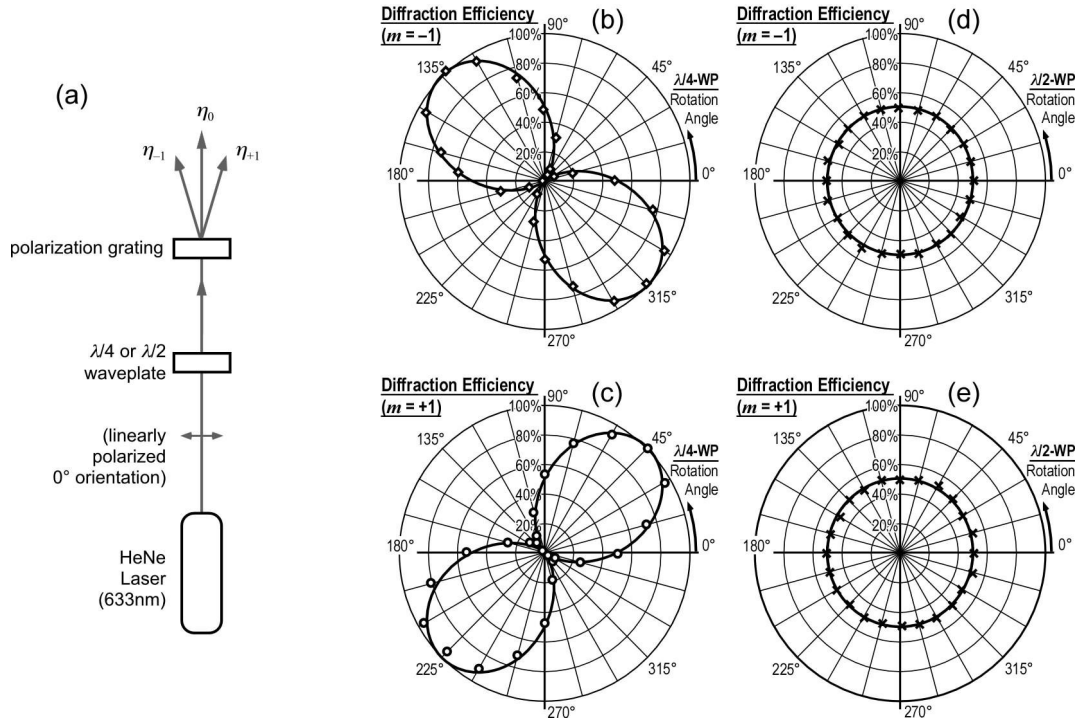


Figure 4. Polarization sensitivity of the reactive mesogen PGs: (a) Measurement setup including a linearly polarized laser with waveplates modulating the polarization incident on the PG; (b) Measured -1 -order and (c) $+1$ -order diffraction response to the rotation of a quarter-waveplate, showing strong experimental sensitivity (from $\sim 0\%$ to $\sim 100\%$); (d) Measured -1 -order and (c) $+1$ -order diffraction response to the rotation of a half-waveplate, showing almost constant $\sim 50\%$. Discrete points correspond to experimental data and solid lines correspond to the theoretical response (Eq. 7).

of $\sim 1 \text{ cm}^2$. These were designed such that each PG stage diffracts approximately $1/3$ of the incident light into its respective first-orders, insuring equal signal strength for each measurement. The absorption of the substrates and Fresnel air-glass reflections led to the transmittance $T \approx 0.7$ at 1550 nm .

A near-infrared tunable fiber laser with output-collimator was arranged as the test-source, along with two zero-order quarter-waveplates, as shown in Fig. 6. The six intensities were measured with a photo-diode across 1525 to 1625 nm (slightly more than the C- and L-bands). An infrared-polarizer was used to set the polarization state of the test-light at -22.5° from the horizontal direction (Fig. 7(a)). The normalized Stokes parameters for this fully-polarized test input are therefore $S'_1 = 0.707$, $S'_2 = -0.707$, and $S'_3 = 0$ across the entire wavelength range.

5. RESULTS AND DISCUSSION

The six first-order diffraction intensities were measured for the linearly-polarized test input, and are shown in Fig. 7(b), where the nominal intensity of the tunable laser was set to 0.5 mW for all wavelengths. Using only the four measured intensities identified in Eq. 13, the resulting Stokes parameters from this measured data were calculated and are shown in Fig. 7(c). The measured intensity of the input signal S_0 was within $\pm 5\%$ of the nominal value. The other Stokes parameters S_1 , S_2 , and S_3 were approximately constant, and matched the ideal values within $\pm 5\%$ even in this very preliminary spectropolarimeter setup. The degree-of-polarization ($\sqrt{S_1^2 + S_2^2 + S_3^2}/S_0$) was also calculated from the measured data, and resulted in a value within $\pm 3\%$ of the actual value (100%). A small amount of measurement error was introduced by the use of zero-order quarter-waveplates (instead of truly achromatic waveplates), by the potential non-uniformity in the IR-absorption of the

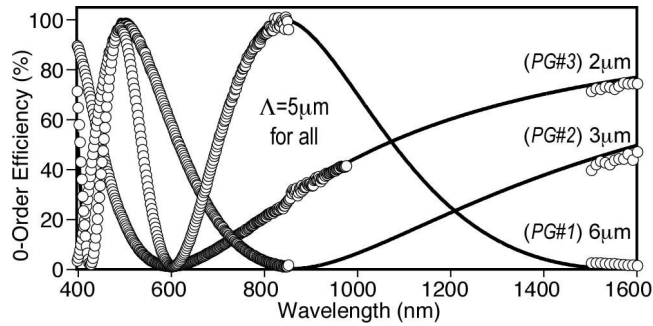


Figure 5. Measured diffraction efficiencies (0-order) of the polarization gratings (PGs) used for the spectropolarimeter implementation. Note that $\Lambda = 5\mu\text{m}$, $\Delta n = 0.144$, and that they were optimized for measurements around 1550 nm.

PG substrates, as well as by the imperfect positioning of the photo-diode that was manually aligned for each measurement.

Nevertheless, the strong correspondence between measurement and actual value clearly demonstrates the ability of this PG spectropolarimeter to *detect all four Stokes parameters in a wavelength-parallel fashion using only four simultaneous intensity measurements*. Its spectral resolution and sampling rate is limited primarily by the implementation of the photo-detection elements, and could most likely be designed with resolution and speed commensurate with conventional spectrometers for the same wavelength range and application (MHz or more). The bandwidth of this detection system is potentially very large, and can be estimated by considering the wavelength range over which all three PGs diffract more than 10% into their first orders ($\Delta\lambda/\lambda_0 \approx 70\%$ of the center wavelength).

While the representative experiment reported here tested a point-light source, it should be noted that one- and two-dimensional (1D/2D) images could also be implemented without much modification. For example, since diffraction occurs in the X-direction (Fig. 2(b)), a linear 1D-source could be arranged along the Y-direction and could be measured directly with the PG polarimeter design already described and appropriate photo-diode arrays. In order to measure the full spectropolarimetric data of a 2D image, a scanning element would be needed to sweep across only one spatial dimension of the input image (e.g. a pushbroom scanner or a rotating mirror). Since each PG stage inherently consolidates the two key functions in spectropolarimetry (wavelength and polarization sensitivity) into a single planar element, a wide variety of polarimeter designs optimized for multi-, hyper-, and imaging polarimetry are possible.

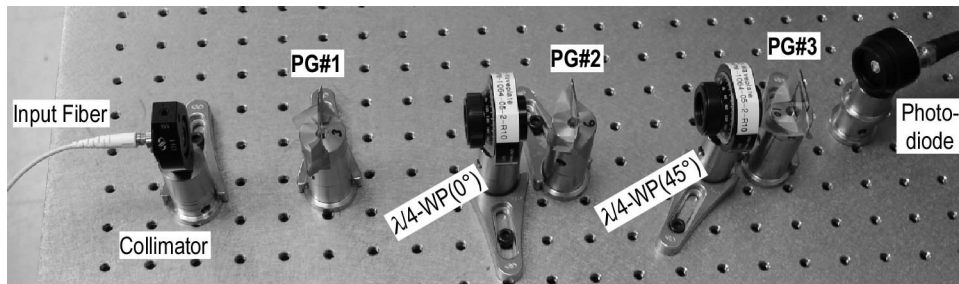


Figure 6. Photograph of the basic spectropolarimeter based on three polarization gratings (PGs) and two quarter-waveplates (WPs). Note that the polarizer used to set the test-input polarization state was placed immediately after the collimator (not shown for clarity).

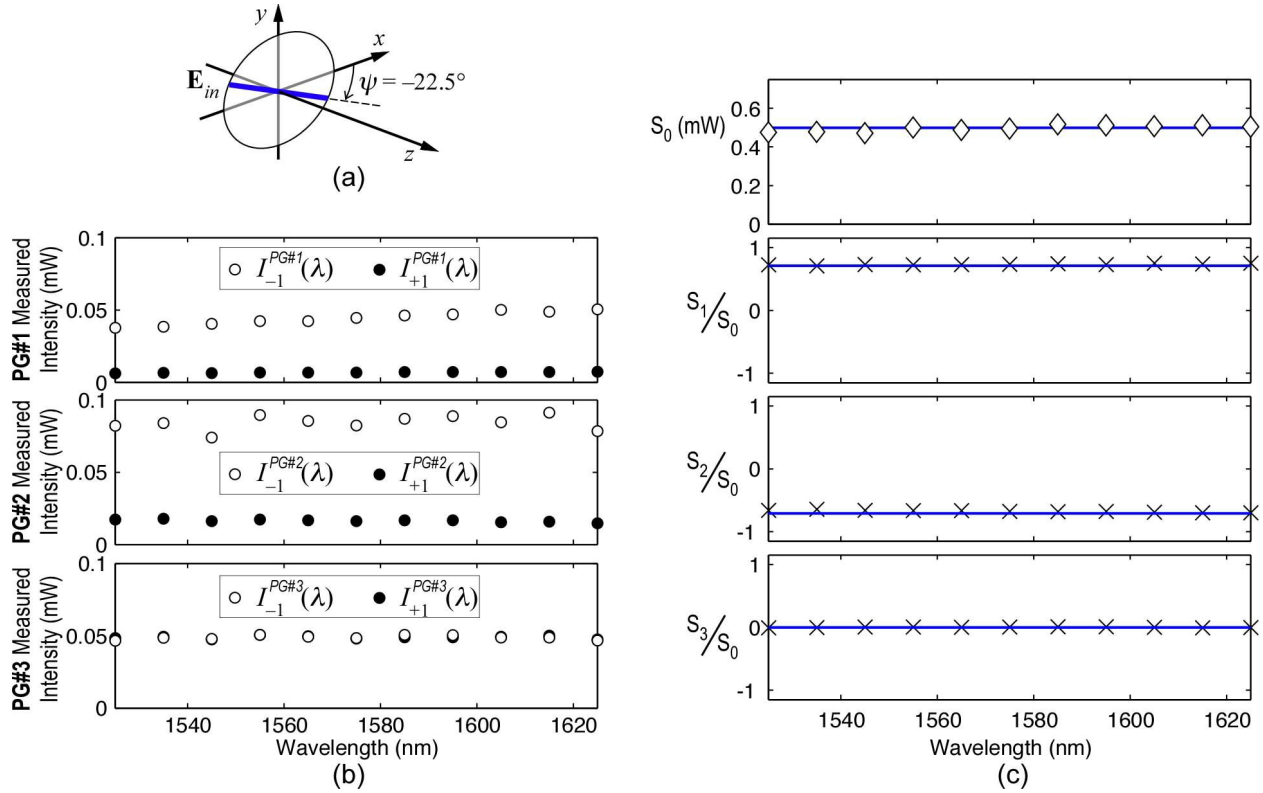


Figure 7. Results of PG spectropolarimeter measuring linearly polarized input light at -22.5° : (a) Input light propagating along Z-direction; (b) Measured first-order intensities; and (c) Measured Stokes parameters calculated only from the four measured intensities $I_{+1}^{PG\#1}(\lambda)$, $I_{-1}^{PG\#1}(\lambda)$, $I_{+1}^{PG\#2}(\lambda)$, and $I_{-1}^{PG\#2}(\lambda)$.

6. CONCLUSIONS

We have proposed a wavelength-parallel spectropolarimeter based on three inline polarization gratings and experimentally demonstrated that it can detect all four Stokes parameters using only four simultaneous intensity measurements per wavelength. Comparative advantages include its simple, robust, and light-weight construction without prisms or traditional polarizers, its ability to be optimized for visible and infrared wavelengths, and its suitability for large-area assembly (if desired). We have also experimentally realized a high-quality polarization grating using reactive mesogens with $\sim 100\%$ diffraction efficiency, strong polarization sensitivity, and very low scattering. When combined with quarter-waveplates, this polarization grating can have ± 1 -order diffraction sensitive to any of the Stokes parameters. Since they consolidate wavelength separation and polarization selectivity, and enable high-speed spectropolarimeters without active tuning elements. The preliminary investigation presented here validates the spectropolarimeter's principle-of-operation, and shows promise that a flexible variety of polarimeter designs optimized for multi-, hyper-, and imaging polarimetry are possible. We anticipate that the simplicity, portability, and improved sensitivity of this spectropolarimeter approach will greatly enhance data collection in astronomy, optical remote sensing, land-mine detection, biomedical imaging, ellipsometry, and optical-fiber links.

ACKNOWLEDGMENTS

This work forms part of the research program of the Dutch Polymer Institute (DPI, projects #298 and #304), and additionally was supported in part by the Department of Electrical and Computer Engineering at NC State University. The authors are grateful to John Muth for the access to the near-infrared source and detector.

REFERENCES

1. F. Gori, "Measuring stokes parameters by means of a polarization grating," *Optics Letters* **24**(9), pp. 584–586, 1999.
2. T. Todorov and L. Nikolova, "Spectrophotopolarimeter: fast simultaneous real-time measurement of light parameters," *Optics Letters* **17**, pp. 358–359, 1992.
3. R. M. A. Azzam, A. M. El-Saba, and M. A. G. Abushagur, "Spectrophotopolarimeter based on multiple reflections in a coated dielectric slab," *Thin Solid Films* **313-314**, pp. 53–57, 1998.
4. G. Cincotti, "Polarization gratings: Design and applications," *IEEE Journal of Quantum Electronics* **39**(12), pp. 1645–1652, 2003.
5. E. Masetti and A. Krasilnikova, "Development and test of a new grating-polarimeter and its application in ellipsometric measurements," *Thin Solid Films* **455-456**, pp. 138–142, 2004.
6. C. Provenzano, G. Cipparrone, and A. Mazzulla, "Photopolarimeter based on two gratings recorded in thin organic films," *Applied Optics* **45**(17), pp. 3929–3934, 2006.
7. E. Collett, *Polarized Light*, Marcel Dekker Inc., New York, 1993.
8. L. Nikolova and T. Todorov, "Diffraction efficiency and selectivity of polarization holographic recording," *Optica Acta* **31**, pp. 579–588, 1984.
9. J. Tervo and J. Turunen, "Paraxial-domain diffractive elements with 100% efficiency based on polarization gratings," *Optics Letters* **25**(11), pp. 785–786, 2000.
10. I. Naydenova, L. Nikolova, T. Todorov, N. C. R. Holme, P. S. Ramanujam, and S. Hvilsted, "Diffraction from polarization holographic gratings with surface relief in side-chain azobenzene polyesters," *Journal of the Optical Society of America B* **15**(4), p. 1257, 1998.
11. G. Cipparrone, A. Mazzulla, S. P. Palto, S. G. Yudin, and L. M. Blinov, "Permanent polarization gratings in photosensitive langmuir blotter films," *Applied Physics Letters* **77**, pp. 2106–2108, 2000.
12. M. J. Escuti and W. M. Jones, "A polarization-independent liquid crystal spatial-light-modulator," *Proc. SPIE - Optics & Photonics Conference* **6332**, p. #22, 2006.
13. M. G. Moharam and L. Young, "Criterion for bragg and raman-nath diffraction regimes," *Applied Optics* **17**(11), pp. 1757–1759, 1978.
14. L. Nikolova, T. Todorov, M. Ivanov, F. Andruzzi, S. Hvilsted, and P. S. Ramanujam, "Polarization holographic gratings in side-chain azobenzene polyesters with linear and circular photoanisotropy," *Applied Optics* **35**(20), pp. 3835–3840, 1996.
15. R. H. Berg, S. Hvilsted, and P. S. Ramanujam, "Peptide oligomers for holographic storage," *Nature* **383**, pp. 505–508, 1996.
16. N. Viswanathan, D. Kim, S. Bian, J. Williams, W. Liu, L. Li, L. Samuelson, J. Kumar, and S. Tripathy, "Surface relief structures on azo polymer films," *Journal of Material Chemistry* **9**, pp. 1941–1955, 1999.
17. S. Slussarenko, O. Francescangeli, and F. Simoni, "High resolution polarization gratings in liquid crystals," *Applied Physics Letters* **71**(25), pp. 3613–3615, 1997.
18. H. Ono, A. Emoto, F. Takahashi, N. Kawatsuki, and T. Hasegawa, "Highly stable polarization gratings in photocrosslinkable polymer liquid crystals," *Journal of Applied Physics* **94**(3), pp. 1298–1303, 2003.
19. Z. Bomzon, G. Biener, V. Kleiner, and E. Hasman, "Spatial fourier-transform polarimetry using space-variant subwavelength metal-stripe polarizers," *Optics Letters* **26**, pp. 1711–1713, 2001.
20. J. Eakin, Y. Xie, R. Pelcovits, M. D. Radcliffe, and G. Crawford, "Zero voltage freedericksz transition in periodically aligned liquid crystals," *Applied Physics Letters* **85**(10), pp. 1671–1673, 2004.
21. J. Chen, P. J. Bos, H. Vithana, and D. L. Johnson, "An electro-optically controlled liquid crystal diffraction grating," *Applied Physics Letters* **67**(18), pp. 2588–2590, 1995.
22. B. Wen, G. Rolfe, and C. Rosenblatt, "Nematic liquid-crystal polarization gratings by modification of surface alignment," *Applied Optics* **41**, pp. 1246–1250, 2002.
23. M. Honma, K. Yamamoto, and T. Nose, "Periodic reverse-twist nematic domains obtained by microrubbing patterns," *Journal of Applied Physics* **96**(10), pp. 5415–5419, 2004.
24. C. M. Titus and P. J. Bos, "Efficient, polarization-independent, reflective liquid crystal phase grating," *Applied Physics Letters* **71**(16), pp. 2239–2241, 1997.

25. B. Wang, X. Wang, and P. J. Bos, "Finite-difference time-domain calculations of a liquid-crystal-based switchable bragg grating," *Journal of the Optical Society of America A* **21**(6), pp. 1066–1072, 2004.
26. Y. Zhang, B. Wang, D. B. Chung, J. Colegrove, and P. J. Bos, "Reflective polarization independent lc phase modulator with polymer wall," *SID Digest* **36**, pp. 1178–1181, 2005.
27. H. Sarkissian, J. B. Park, B. Y. Zeldovich, and N. V. Tabirian, "Potential application of periodically aligned liquid crystal cell for projection displays," *Proc. of CLEO/QELS Baltimore MD*, p. poster JThE12, 2005.
28. J. Tervo, V. Kettunen, M. Honkanen, and J. Turunen, "Design of space-variant diffractive polarization elements," *Journal of the Optical Society of America A* **20**(2), pp. 282–289, 2003.
29. G. Crawford, J. Eakin, M. D. Radcliffe, A. Callan-Jones, and R. Pelcovits, "Liquid-crystal diffraction gratings using polarization holography alignment techniques," *Journal of Applied Physics* **98**, p. 123102, 2005.
30. M. Schadt, H. Seiberle, and A. Schuster, "Optical patterning of multi-domain liquid-crystal displays with wide viewing angles," *Nature* **381**, pp. 212–215, 1996.
31. H.-S. Kwok, V. G. Chigrinov, H. Takada, and H. Takatsu, "New developments in liquid crystal photo-aligning by azo-dyes," *IEEE/OSA Journal of Display Technology* **1**(1), pp. 41–50, 2005.
32. R. A. M. Hikmet, J. Lub, and D. J. Broer, "Anisotropic networks formed by photopolymerization of liquid-crystalline molecules," *Advanced Materials* **3**(7/8), pp. 392–394, 1991.
33. D. J. Broer, "Photoinitiated polymerization and crosslinking of liquid-crystalline systems," in *Radiation Curing in Polymer Science and Technology Vol. 3: Polymerisation Mechanisms*, J.-P. Fouassier and J. Rabek, eds., **3**, pp. Ch. 12, 383–443, Elsevier Science, London, 1993.
34. D. J. Broer, G. N. Mol, J. A. M. M. van Haaren, and J. Lub, "Photo-induced diffusion in polymerizing chiral-nematic media," *Advanced Materials* **11**(7), pp. 573–, 1999.
35. J. Lub, P. van de Witte, C. Doornkamp, J. P. A. Vogels, and R. T. Wegh, "Stable photopatterned cholesteric layers made by photoisomerization and subsequent photopolymerization for use as color filters in liquid-crystal displays," *Advanced Materials* **15**, pp. 1420–1425, 2003.
36. H. Sarkissian, S. V. Serak, N. Tabirian, L. B. Glebov, V. Rotar, and B. Y. Zeldovich, "Polarization-controlled switching between diffraction orders in transverse-periodically aligned nematic liquid crystals," *Optics Letters* **31**, pp. 2248–2250, 2006.